



저작자표시-비영리-변경금지 2.0 대한민국

이용자는 아래의 조건을 따르는 경우에 한하여 자유롭게

- 이 저작물을 복제, 배포, 전송, 전시, 공연 및 방송할 수 있습니다.

다음과 같은 조건을 따라야 합니다:



저작자표시. 귀하는 원저작자를 표시하여야 합니다.



비영리. 귀하는 이 저작물을 영리 목적으로 이용할 수 없습니다.



변경금지. 귀하는 이 저작물을 개작, 변형 또는 가공할 수 없습니다.

- 귀하는, 이 저작물의 재이용이나 배포의 경우, 이 저작물에 적용된 이용허락조건을 명확하게 나타내어야 합니다.
- 저작권자로부터 별도의 허가를 받으면 이러한 조건들은 적용되지 않습니다.

저작권법에 따른 이용자의 권리는 위의 내용에 의하여 영향을 받지 않습니다.

이것은 [이용허락규약\(Legal Code\)](#)을 이해하기 쉽게 요약한 것입니다.

[Disclaimer](#)

의학박사 학위논문

췌장암 동물 모델에서 고강도
집속 초음파와 Gemcitabine 병용
요법의 효과에 대한 연구

2013년 2월

서울대학교 대학원

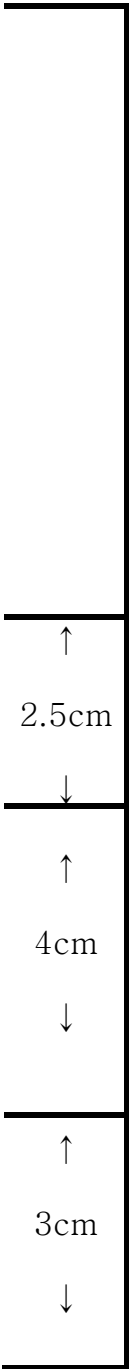
의학과 영상의학 전공

이은선

체강암 동물 모델에서 고강도 집속 초음파와
Gemcitabine 병용 요법의 효과에 대한 연구

2013년

이은선



의학박사 학위논문

췌장암 동물 모델에서 고강도
집속 초음파와 Gemcitabine 병용
요법의 효과에 대한 연구

2013년 2월

서울대학교 대학원

의학과 영상의학 전공

이 은 선

The Ph.D. thesis

Concurrent Pulsed High-Intensity
Focused Ultrasound and Gemcitabine
Treatment in Animal Models of
Pancreatic Cancer

February 2013

Seoul National University

College of Medicine, Radiology

LEE Eun Sun

췌장암 동물 모델에서 고강도 집속 초음파와 Gemcitabine 병용 요법의 효과에 대한 연구

지도 교수 이 재 영

이 논문을 의학박사 학위논문으로 제출함

2012년 10월

서울대학교 대학원

의학과 영상의학 전공

이 은 선

이은선의 의학박사 학위논문을 인준함

2012년 12월

위원장	<u>최 병 인</u>	(인)
부위원장	<u>이 재 영</u>	(인)
위원	<u>김 용 태</u>	(인)
위원	<u>류 지 곤</u>	(인)
위원	<u>김 영 선</u>	(인)

학위논문 원문제공 서비스에 대한 동의서

본인의 학위논문에 대하여 서울대학교가 아래와 같이 학위논문 제공하는 것에 동의합니다.

1. 동의사항

- ① 본인의 논문을 보존이나 인터넷 등을 통한 온라인 서비스 목적으로 복제할 경우 저작물의 내용을 변경하지 않는 범위 내에서의 복제를 허용합니다.
- ② 본인의 논문을 디지털화하여 인터넷 등 정보통신망을 통한 논문의 일부 또는 전부의 복제, 배포 및 전송 시 무료로 제공하는 것에 동의합니다.

2. 개인(저작자)의 의무

본 논문의 저작권을 타인에게 양도하거나 또는 출판을 허락하는 등 동의 내용을 변경하고자 할 때는 소속대학(원)에 공개의 유보 또는 해지를 즉시 통보하겠습니다.

3. 서울대학교의 의무

- ① 서울대학교는 본 논문을 외부에 제공할 경우 저작권 보호장치(DRM)를 사용하여야 합니다.
- ② 서울대학교는 본 논문에 대한 공개의 유보나 해지 신청 시 즉시 처리해야 합니다.

논문제목: 채장암 동물 모델에서 고강도 집속 초음파와 Gemcitabine 병용 요법의 효과에 대한 연구

학위구분 : 석사 □ · 박사 ■

학 과 : 의학과 영상의학

학 번 : 2011-30570

연 락 처 :

저 작 자 : 이 은 선 (인)

제 출 일 : 2013 년 2 월 일

서울대학교총장 귀하

ABSTRACT

Introduction: We sought to investigate whether concurrent exposure to pulsed high-intensity focused ultrasound (HIFU) and the chemotherapeutic drug gemcitabine could enhance apoptosis in pancreatic cancer.

Methods: A pancreatic cancer xenograft model was established using BALB/c nude mice and human pancreatic cancer cells (PANC-1). In the first study, mice were randomly allocated into one of the following four groups: control (n = 4), HIFU alone (n = 4), gemcitabine alone (GEM) (n = 28), and concurrent treatment of HIFU with gemcitabine (HIGEM) (n = 28). The GEM and HIGEM groups were subdivided into four subgroups according to the injected drug dose (50 - 200 mg/kg) in 16 mice and another four subgroups

according to the time interval between drug injection and HIFU treatment in 16 mice (each subgroup, $n = 4$). Apoptotic ratios were evaluated using the terminal deoxynucleotidyl transferase-mediated dUTP nick end-labeling (TUNEL) assay and percentage of necrosis, as evaluated with Harris hematoxylin solution and eosin Y (H & E) staining, three days after treatment. The second study was performed to evaluate tumor growth rates of the four groups. Each group was treated weekly for three weeks, and the tumor size was periodically measured for up to four weeks from the beginning of treatment.

Results: In the first study, the overall apoptotic ratios in the HIGEM group were significantly higher than the GEM group ($p = 0.02$). In a subgroup analysis, HIGEM was superior to GEM in generating apoptosis when 150-200 mg/kg gemcitabine and short-term intervals less than 2 hours were used ($p = 0.01$). In the second study, HIGEM treatment exhibited the slowest tumor growth. However, despite a visible distinction, no statistically significant difference was found between HIGEM and GEM groups ($p > 0.05$).

Conclusion: Treatment with both HIFU and gemcitabine might enhance cell apoptosis and reduce tumor growth in pancreatic carcinoma. For this concurrent treatment, high dosage of gemcitabine with a short-term delay would be recommended to maximize therapeutic effect.

Key words

High-Intensity Focused Ultrasound Ablation

Pancreatic Neoplasms

Gemcitabine

Animal study

Student Number: 2011-30570

목차

영문초록.....	i
목차.....	iv
List of Tables.....	v
List of Figures.....	vi
Introduction.....	1
Materials and Methods.....	4
Results.....	11
Discussion.....	15
Acknowledgement.....	21
Tables.....	22
Figures.....	26
References.....	39
Appendix.....	47
국문초록.....	55

List of Tables

Table 1. Apoptotic ratio according to dosage of gemcitabine.....22

Table 2. Apoptotic ratio according to treatment interval between gemcitabine
and high-intensity focused ultrasound.....23

Table 3. Gross necrosis according to dosage of gemcitabine.....24

Table 4. Gross necrosis according to treatment interval between gemcitabine
and high-intensity focused ultrasound.....25

List of Figures

Figure 1. Phantom study performed for the selection of optimal conditions for low-energy HIFU therapy.....	26
Figure 2. The pancreatic cancer xenograft nude mouse model.....	28
Figure 3. The flowcharts of the animal study.....	29
Figure 4. Box plots of the apoptotic ratio (%) according to the treatment.....	30
Figure 5. A paired t-test between concurrent HIFU and gemcitabine treatment.....	33
Figure 6. Fluorescent TUNEL assay with DAPI staining in single time treatment group.....	34

Figure 7. Line graph of serial changes in volume ratio (tumor volume at day 28/ tumor volume at day 0).....36

Figure 8. Box plots of volume ratio (tumor volume at day 28/ tumor volume at day 0) according to treatment after weekly treatment for 3 consecutive weeks.....37

Introduction

Pancreatic cancer is the fourth most common cause of cancer-related mortality worldwide, with incidence equaling mortality (1). The majority of patients with pancreatic cancer present with locally advanced or metastatic disease that is inoperable (2). Gemcitabine has been the first-line treatment for advanced pancreatic cancer over the past decade and has significantly improved the median overall survival (3, 4). However, the prognosis of pancreatic cancer is still dismal, with less than 6% 5-year relative survival in the United States for 2002-2008 (<http://seer.cancer.gov/statfacts>).

High-intensity focused ultrasound (HIFU) therapy is an emerging therapeutic modality that uses ultrasound waves as carriers of energy. HIFU is now being clinically used or investigated as a truly non-invasive local treatment to treat solid tumors in various organs, such as the uterus, prostate, bone, liver, and pancreas (5-13). Tissue damage by HIFU can be caused by mechanical injury due to inertial cavitation, shear force and micro-streaming in addition to thermal injury (10). HIFU is also well known for enhancing drug delivery to targeted tumors with low energy by sonoporation (14-18).

Therefore, concurrent treatment with HIFU and systemic chemotherapy has been tried with several types of tumors in clinical trials (19-24).

The concurrent use of HIFU and systemic chemotherapy has also been tried in unresectable pancreatic cancer with gemcitabine to improve the dismal prognosis mentioned above (19, 22), and promising results have been reported. However, these studies did not provide any data to compare concurrent HIFU and systemic chemotherapy treatment with systemic chemotherapy alone. Furthermore, their treatment protocols varied too widely to provide conclusions about an optimal treatment protocol. To the best of our knowledge, no animal studies have been performed to address this issue. Although Wang et al. (25) reported the effects of endostatin and gemcitabine combined with HIFU in a murine xenograft model of human pancreatic cancer, it was not a study of concurrent therapy with HIFU and chemotherapeutic drugs. Rather, it studied combined treatment with endostatin and gemcitabine because all tumors without a control group were only treated with HIFU on the last day of a 4-week period of systemic chemotherapy.

Thus, the purposes of our study were to experimentally investigate whether concurrent treatment with HIFU and systemic chemotherapy could enhance

apoptosis in pancreatic cancer tumors and to identify the most optimal therapeutic protocol.

Materials and Methods

Our Institutional Animal Care and Use Committee approved this animal study (IACUC No. 11-0147).

Phantom study

To determine HIFU parameters in the animal study, a study using tissue phantoms was performed with varying HIFU parameters. The tissue phantom consists of distilled water, bovine serum albumin, corn syrup, Tris buffer, acrylamide, glass beads, ammonium persulfate solution and tetramethylethylenediamine. Acoustic power (20-200 W), exposure time (9-36 s), pulses per treatment spot (60-120), duty cycle (50%) and pulse repetition frequency (3.3 Hz) were used in different combinations. The condition under which the most acoustic cavitations occurred without gross coagulation necrosis was used for in vivo experiments (Fig. 1).

Animals

Human pancreatic cancer cells (PANC-1) in logarithmic phase were added to DMEM (Dulbecco's modified Eagle medium) containing 10% FBS

(fetal bovine serum) and 1% penicillin after digestion with 0.25% trypsin at 37°C, and the cell concentration was adjusted to $5 \times 10^6/\text{mL}$ with normal saline. Subsequently, 0.2 mL of cell suspension was inoculated in bilateral or unilateral thighs of BALB/c nude mice with sterile syringes, and tumors were grown until they reached an approximate ($\pm 20\%$) size of 200-500 mm³. In this way, the animal xenograft model of human pancreatic cancer was established (Fig. 2). Intra-peritoneal general anesthesia was performed using a mixture of Zoletil[®] (30 mg/kg) and Rompun[®] (10 mg/kg) before HIFU therapy.

HIFU Equipment

The FEP-BY02TM HIFU unit (Yuande Biomedical Engineering Limited Corporation, Beijing, China) was used throughout this study. The therapeutic HIFU transducer is a fixed focus concave transducer composed of 251 piezoelectric elements with an overall aperture of 37 cm and a focal length of 26 cm. The elements of this transducer are driven in phase at a frequency of 1.04 MHz. The focal zone of the therapeutic transducer is an elongated ellipsoid with an axial length of 8 mm (-6 dB) and radial diameter of 3 mm.

The targeted tumor was identified using a 5 MHz imaging transducer (GE Logiq 5, Seongnam, Korea) mounted coaxially to the HIFU therapeutic transducer and positioned in the center of the therapeutic transducer's focal zone.

HIFU Parameters

An HIFU beam was insonated into the tumor and moved automatically from spot to spot in an overlapping manner to treat a volume of tissue with a spacing of 2 mm in the x, y and z dimensions. Treatment parameters were determined by the phantom study as follows: input target power: 50 W; pulses/spot: 60 (18s); pulse repetition frequency: 3.3 Hz; and duty cycle: 50% (transmission time of a unit pulse: 150 ms, and intermission time between pulses: 150 ms).

Experimental protocol

The animal study was categorized into two experiments of 1) single time treatment and tumor apoptosis and 2) repetitive treatment and tumor growth (Fig. 3).

1. Single Time Treatment and Tumor Apoptosis

At least four mice were first randomly allocated into four groups: control group, HIFU alone, gemcitabine alone (GEM), and concurrent treatment with HIFU and gemcitabine (HIGEM). The GEM and HIGEM groups included more mice to investigate differences in tumor apoptosis according to the dose of injected gemcitabine and the time interval between gemcitabine injection and HIFU treatment. Finally, the GEM and HIGEM groups included a total of 28 mice because four different drug doses (50, 100, 150 and 200 mg/kg of gemcitabine and immediate HIFU treatment (4 mice in each) and four different time intervals (immediate and 2-hour, 6-hour, and 24-hour delay in HIFU treatment after 150 mg/kg gemcitabine injection (4 mice in each) were used. Four mice treated with 150 mg/kg gemcitabine followed immediately by HIFU treatment were included in both subgroups (drug dose group and treatment time interval group).

HIFU therapy was given to one side of the tumors in bilateral thighs to compare the treatment efficacy between control and HIFU alone or HIGEM and GEM groups in an individual. The experiment began when the tumors reached approximately 500 mm³ (\pm 20%). The administration of gemcitabine

was performed by intra-peritoneal injection, and the mice were sacrificed 3 days after HIFU therapy, which was reported by prior literature as the best time to identify cell apoptosis (18).

2. Repetitive Treatment and Tumor Growth

To investigate the difference in tumor growth rates among treatment groups, four groups were established: control (n = 2), HIFU only (n = 4), GEM (n = 4) and HIGEM (n = 6) groups. For this study, a xenograft was created on one thigh of a mouse. For GEM and HIGEM groups, the dosage of gemcitabine and the treatment time interval were fixed at 200 mg/kg and 2 hours, respectively, a therapeutic protocol that exhibited the highest apoptotic ratio in our single time treatment study. The experiment was initiated when the tumors reached approximately 100-300 mm³, which were smaller than our single time treatment study to prolong the survival time of mice.

Except for the control group, all mice were treated once a week for 3 consecutive weeks at days 0, 7 and 14 and sacrificed at day 28. For 4 weeks, the width, length, and height of the tumor were measured using ultrasound (Toshiba Aplio XG TM, Tokyo, Japan) by one author (L.E.S.) at days 0, 7, 14,

19, 26, and 28, and tumor volume was calculated by the following formula:

$$Volume (mm^3) = \pi/6 \times width (mm) \times length (mm) \times height (mm)$$

Histopathologic study

Tissue sections (4 μ m) were prepared using a microtome, placed on glass slides, and stained with Harris hematoxylin solution and eosin Y (H&E) (Sigma, St. Louis, MO). Necrotic areas were identified under a low-power field (x 20) and scored with a 5% scale system in consensus by two researchers (L.E.S. and K.H.) using multi-viewing microscopy.

Apoptotic cells were quantified by the TUNEL (terminal deoxynucleotidyl transferase-mediated dUTP nick end-labeling) assay, which was performed using the In Situ Cell Death Detection Kit, Fluorescein (Roche, Penzberg, Germany). The fraction of apoptotic cells in a whole tumor visualized under a high-power field (x 200) was calculated by two researchers (K.H. and P.J.) using Image J software (<http://rsbweb.nih.gov/ij>). Each researcher calculated the apoptotic cell fraction in 5 high-power fields randomly and independently, producing 10 values, which were then averaged. In addition, fluorescent DAPI (4', 6-diamidino-2-phenylindole) staining was

performed with TUNEL for the easy identification of apoptotic cells.

Statistical analysis

For all of the in vivo experiments, the results were reported as median values. For single time treatment studies, the percentages of apoptotic cells and gross necrosis were used as measures of the primary outcome in the statistical analyses. In repetitive treatment studies, the tumor volume ratio (that is, tumor volume at a specific day divided by tumor volume at day 0) was used as the primary outcome of the experiment. Statistical analysis was performed using summary statistics, the Kruskal-Wallis test and the paired t-test with MedCalc statistical software, version 12.2.1 (MedCalcSoftware, Mariakerke, Belgium). A P value was considered to be significant when it was < 0.05 .

Results

Phantom study

In HIFU with 20 W of power, no trace of tiny bubbly lesions representing acoustic cavitation was found in the tissue phantom. We found traces of acoustic cavitations at 50 W of input energy, but elliptical cloudy discoloration (which may represent coagulation necrosis) appeared at ≥ 100 W (Fig. 1). Therefore, 50W of input energy was selected as the optimal energy. Finally, the therapeutic HIFU parameters were determined for our animal study as follows: input target power: 50W; pulses/spot: 60 (18s); pulse repetition frequency: 3.3 Hz; and duty cycle: 50% (transmission time of a unit pulse (t1): 150 ms, and intermission time between pulses (t2): 150 ms).

Single Time Treatment and Tumor Apoptosis

Apoptotic ratio

The effect of gemcitabine dosage:

The highest median apoptotic ratio was noted in the HIGEM group with the use of 200 mg/kg of gemcitabine, i.e., 58.02%, with a range from 13.48 to

76.98%. The median, minimum and maximum apoptotic ratios are shown in Table 1. The Kruskal-Wallis test revealed that the HIGEM group showed a significantly higher apoptotic ratio than the GEM group when a high dose of gemcitabine (150 and 200 mg/kg) was used ($p = 0.01$) (Fig. 4A).

The effect of therapeutic time interval between gemcitabine injection and HIFU:

The highest median apoptotic ratio was noted in the HIGEM group with a 2-hour delay, i.e., 49.20%, with a range from 8.08 to 59.14%. The median, minimum and maximum apoptotic ratios are shown in Table 2. The Kruskal-Wallis test revealed that the HIGEM group showed a significantly higher apoptotic ratio than the GEM group with a short-term delay (immediate and 2-hour delay) ($p = 0.008$) (Fig. 4B). When HIGEM groups ($n = 32$) were compared with corresponding GEM groups, regardless of gemcitabine dosage and treatment interval, a paired t-test revealed that apoptotic ratios in the HIGEM group were significantly higher than the GEM group ($p = 0.02$) (Fig. 5).

Gross tumor necrosis

The effect of gemcitabine dosage:

The highest median value of gross necrosis was noted in the HIGEM group when 200 mg/kg of gemcitabine was used, i.e., 45%, with a range from 5 to 60%. The median, minimum and maximum percentages of gross necrosis are shown in Table 3. However, the Kruskal-Wallis test showed no significant difference between all four subgroups, regardless of treatment group or gemcitabine dosage ($p > 0.05$).

The effect of therapeutic time interval between gemcitabine injection and HIFU:

The highest median value of gross necrosis was noted in the concurrent therapy group (HIGEM) with a 2-hour delay, i.e., 32.5%, with a range from 0 to 60%. The median, minimum and maximum apoptotic ratios are shown in Table 4. However, the Kruskal-Wallis test showed no significant difference between any of the subgroups according to the type of treatment or therapeutic time interval between gemcitabine injection and HIFU ($p > 0.05$).

Repetitive Treatment and Tumor Growth

In all four treatment groups, tumor growth increased with time (Fig. 7). Tumors in control and HIFU groups gradually increased from the beginning, whereas tumors in the GEM and HIGEM groups were suppressed during the treatment period and showed growth spurts in the last week. Tumors in the HIGEM groups were the slowest growing tumors among the four groups (Fig. 7). The Kruskal-Wallis test showed that the HIGEM group had significantly slower tumor growth than the control and HIFU alone groups. However, despite a visible distinction, no statistically significant difference existed between GEM and HIGEM groups (Fig. 8).

Discussion

Therapeutic ultrasound relies on thermal or mechanical effects to induce reversible or irreversible changes in tissue. The mechanical effects of ultrasound include acoustic streaming and the effect of acoustic radiation force on particles, but they are often dominated by acoustic cavitation, which refers to oscillations of gas bubbles in an ultrasonic field (26). These bubbles either repeat radial oscillations in a resonant size with the insonated frequency (stable cavitation; noninertial cavitation) or oscillate in a similar manner, expanding gradually above their resonant size due to net influxes of vapor into the bubbles (rectified diffusion) and finally disintegrating by a violent and asymmetrical collapse (unstable cavitation; inertial cavitation) (17). Stable cavitation has previously been reported to enhance facilitating thrombolysis (27), the delivery of drugs to the vascular endothelium (28) and enabling the reversible opening of the blood–brain barrier for drug delivery to the nervous system (29). Inertial cavitation has been demonstrated to enhance heat deposition to thermally ablate tumors (17) and increase the permeability of cellular membranes to large molecules, a process known as sonoporation (30).

A recent in vitro study demonstrated that sonoporation by inertial cavitation can be exploited for the delivery of macromolecules into an obstructed vessel, and it established a direct correlation between acoustic emissions associated with inertial cavitation and the amount of drug being delivered (31). Several in vitro and in vivo studies also suggested that sonoporation could enhance drug delivery through making microvessels porous and inducing the extravasation of macromolecular anticancer agents into the tumor (28, 30-39).

In our study, HIGEM groups showed better performance than corresponding GEM groups in inducing the apoptosis of cancer cells with a high dose (150 and 200 mg/kg) of gemcitabine and a short-term (0- and 2-hour) delay. However, HIGEM groups did not show any significant difference in apoptotic ratios at a low dose (50 and 100 mg/kg) or long-term (6- and 24-hour) delays compared to corresponding GEM groups. These results suggest that concurrent treatment with drugs and HIFU requires a proper drug dose and treatment interval to enhance tumor apoptosis above a drug-only treatment. Given that a prior article (40) reported that a cell membrane resealing process occurs in vitro within a few seconds after sonoporation by lysosomal-associated membrane protein (LAMP-1) expression, no significant

difference between HIGEM and GEM in long-term (6 and 24-hour) delay groups could be easily accepted because most transient pores might have finished their repair process by that time. The more remaining pores, the better synergism can exist. However, it was unexpected that the 2-hour delay groups would show higher median apoptosis than immediate groups. Slow drug distribution through intra-peritoneal drug injection in our experiment could be a possible cause.

The results described above reveal that the enhancement of cell apoptosis by the addition of HIFU to drug treatment is not just an added effect but also a synergistic effect by increasing drug delivery through sonoporation. If no synergism existed between these therapies, the results should be similar regardless of varying interval times. Based on these results, we can suggest that the therapeutic power could be maximized through the adjustment and optimization of therapeutic protocols in concurrent treatments.

Our repetitive treatments on tumor growth rate of the four treatment groups showed visible differences between four treatment groups, with the HIGEM group showing the slowest growth rate. Analyzing the results of the repetitive treatment study in detail, tumor sizes in the control and HIFU

groups gradually increased from the beginning, whereas the tumors in the GEM and HIGEM groups were suppressed during the treatment period and showed growth spurts in the last week, as shown on the line graph (Fig. 7). The growth suppression during treatment followed by a growth spurt after loss of the treatment effect was a predictable result.

However, in the HIFU alone group of our repetitive treatment, the gradual growing trend during treatment needs some interpretation. One possible reason is the effect of using low input power (50 W) without systemic chemotherapy. When HIFU is used as an anti-cancer treatment independently, high input power within a range of 140 to 400 W has been used in most of clinical cases (5, 8, 9) for obtaining coagulation necrosis in the literature. However, in our study, the low input power of 50 W was used consistently, even in HIFU-only therapy, which was insufficient for independently resulting in solid coagulation necrosis. Although a low input energy of 50 W most likely resulted in insufficient therapeutic power in the HIFU alone treatment, it was more appropriate to use as low an input power as possible in our study because our first goal was to utilize the synergism between HIFU and

systemic chemotherapy by using the mechanism of sonoporation in the drug delivery phase.

Another advantage of concurrent HIFU and systemic chemotherapy is a lower complication rate. According to the recent literature by Jung et al (41), the most common complications of HIFU in pancreatic cancer were skin burns and vertebral fat necrosis in the beam pathway. In their report, skin burns and vertebral necrosis developed in all 35 patients, and subcutaneous fat necrosis developed in 10 patients following HIFU with 120-350 W of power. However, in our animal experiment, no significant skin change developed after HIFU therapy, except in cases of mistargeting due to unexpected movement under the semi-anesthetic. This lack of skin effects was most likely due to the use of low input power. Considering that the thickness of the skin in nude mice is much thinner than that of humans, the risk of HIFU-related complications would be negligible in humans if concurrent treatment with drug and HIFU was applied with a similar low-input HIFU power. Therefore, we expect that the concurrent treatment of pancreatic cancer patients with low input power, such as that used in our experiments, might have an effect on

enhancing the drug delivery of systemic chemo-agents and reducing HIFU-related complications.

There are several limitations in our study. The major limitation was the small number of animals in each group. This could unfavorably influence the statistical analysis in our study, even though our studies showed a relatively consistent tendency. Second, only indirect histopathologic evidence of enhanced drug delivery was reported for apoptotic ratios by TUNEL assay. Apoptosis is a physiologically essential mechanism of cells and plays an important role in reducing the development and progression of tumors. An appealing strategy for cancer therapy is to target the lesions that induce apoptosis in cancer cells (42). Therefore, we evaluated apoptosis as a primary outcome through single time treatment and repetitive treatment studies. However, if possible, further in vivo studies like the prior in vitro study (31) would be needed to establish a direct correlation by quantitative analysis between sonoporation and drug delivery. Third, we observed tumor growth for only one month in our repetitive treatment study, according to our original plan. However, as our line graph shows in figure. 7, longer observations should have been performed to evaluate whether the tumor growth ratio in the

HIGEM group would become more different from the GEM group. Finally, human pancreatic tumors are larger and more deeply located than those of animal xenograft models. Therefore, the re-optimization of HIFU parameters might be needed when the concurrent treatment clinically applies to pancreatic cancer patients.

In conclusion, concurrent HIFU and gemcitabine treatment could be an effective and truly non-invasive treatment, which might enable enhanced cell apoptosis and reduce the tumor growth in pancreatic carcinoma. Under low HIFU energy input conditions, the use of high dosage of gemcitabine with a short-term delay would be recommended to maximize therapeutic effect.

Acknowledgements

This study is partly supported by Basic Science Research Program through the National Research Foundation of Korea (NRF) funded by the Ministry of Education, Science and Technology (2012010930).

Tables

Table 1. Apoptotic Ratio according to Dosage of Gemcitabine

	Control	HIFU only	HIGEM 50 mg/kg	GEM 50 mg/kg	HIGEM 100 mg/kg	GEM 100 mg/kg	HIGEM 150 mg/kg	GEM 150 mg/kg	HIGEM 200 mg/kg	GEM 200 mg/kg
Median (%)	0.83	27.89	21.78	16.23	26.61	26.16	40.06	25.50	58.02*	13.25
Minimum (%)	0.53	4.16	10.79	3.64	13.40	7.61	15.82	4.86	13.48	2.14
Maximum (%)	1.22	47.09	39.00	36.50	52.92	55.80	60.31	43.68	76.98	68.06

*HIFU: high-intensity focused ultrasound, GEM: gemcitabine, HIGEM: concurrent treatment with HIFU and gemcitabine; there were four mice in each group. * The highest median value*

Table 2. Apoptotic Ratio according to Treatment Interval between Gemcitabine and High-Intensity Focused Ultrasound

			HIGEM	GEM	HIGEM	GEM	HIGEM	GEM	HIGEM	GEM
	Control	HIFU only	Imm	Imm	2 H	2 H	6 H	6 H	24 H	24 H
Median (%)	0.83	27.89	40.06	25.50	49.20*	9.16	33.92	23.56	23.23	26.31
Minimum (%)	0.53	4.16	15.82	4.86	8.08	1.22	6.36	5.80	8.11	8.02
Maximum (%)	1.22	47.09	60.31	43.68	59.14	41.68	49.29	56.10	55.43	48.54

HIFU: high-intensity focused ultrasound, GEM: gemcitabine, HIGEM: concurrent treatment of HIFU and gemcitabine, Imm: immediately, H: delayed hours after gemcitabine injection to HIFU treatment

*There were four mice in each group. * The highest median value*

Table 3. Gross Necrosis according to Dosage of Gemcitabine

	Control	HIFU only	HIGEM 50 mg/kg	GEM 50 mg/kg	HIGEM 100 mg/kg	GEM 100 mg/kg	HIGEM 150 mg/kg	GEM 150 mg/kg	HIGEM 200 mg/kg	GEM 200 mg/kg
Median (%)	0	15	15	0	35	27.5	10	20	45*	40
Minimum (%)	0	10	0	0	0	0	5	0	5	5
Maximum (%)	0	20	30	70	50	60	30	35	60	60

*HIFU: high-intensity focused ultrasound, GEM: gemcitabine, HIGEM: concurrent treatment of HIFU and gemcitabine; there were four mice in each group. * The highest median value*

Table 4. Gross Necrosis according to Treatment Interval between Gemcitabine and High-Intensity Focused Ultrasound

			HIGEM	GEM	HIGEM	GEM	HIGEM	GEM	HIGEM	GEM
	Control	HIFU only	Imm	Imm	2 H	2 H	6 H	6 H	24 H	24 H
Median (%)	0	15	10	20	32.5*	2.5	10	5	2.5	5
Minimum (%)	0	10	5	0	0	0	0	0	0	0
Maximum (%)	0	20	30	35	60	20	65	50	10	20

HIFU: high-intensity focused ultrasound, GEM: gemcitabine, HIGEM: concurrent treatment with HIFU and gemcitabine,

Imm: immediately, H: delayed hours after gemcitabine injection to HIFU treatment

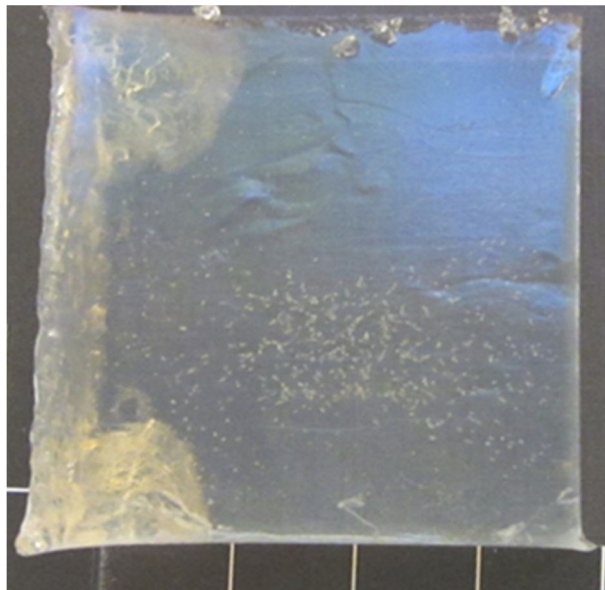
*There were four mice in each group. * The highest median value*

Figures

Fig. 1. Phantom study performed for the selection of optimal conditions for low-energy HIFU therapy, resulting in acoustic cavitations only, not coagulation necrosis.

**HIFU: high-intensity focused ultrasound*

- A. Formation of tiny bubbly lesions representing acoustic cavitations without coagulation necrosis (input target power: 50W; pulses/spot: 60 (18s); pulse repetition frequency: 3.3 Hz; and duty cycle: 50%)



B. Formation of elliptical cloudy discoloration representing coagulation necrosis surrounded by acoustic cavitations (input target power: 100W; pulses/spot: 60 (18s); pulse repetition frequency: 3.3 Hz; and duty cycle: 50%)

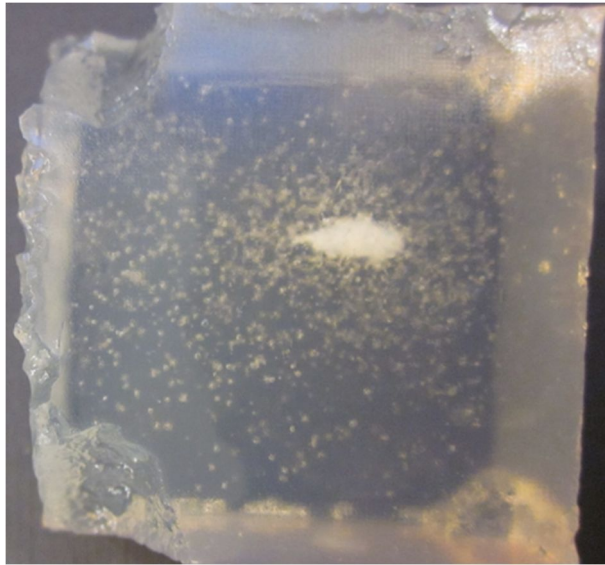


Fig. 2. The pancreatic cancer xenograft nude mouse model of human pancreatic cancer cell (PANC-1) tumors on bilateral thighs.

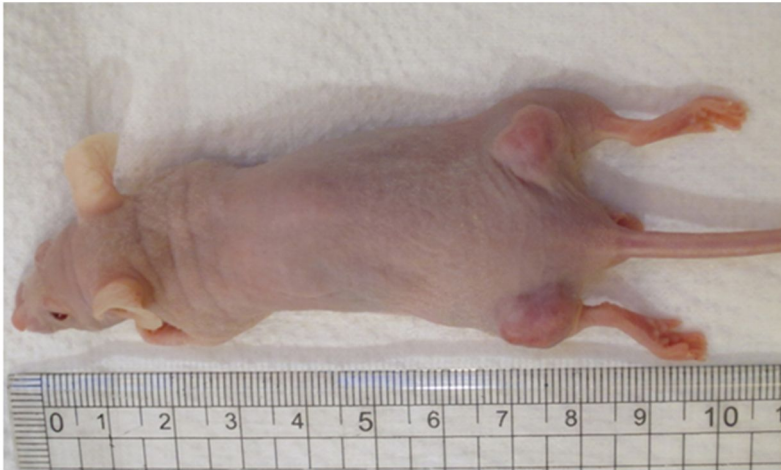


Fig. 3. The animal study was categorized into two experiments of 1) single time treatment and tumor apoptosis and 2) repetitive treatment and tumor growth.

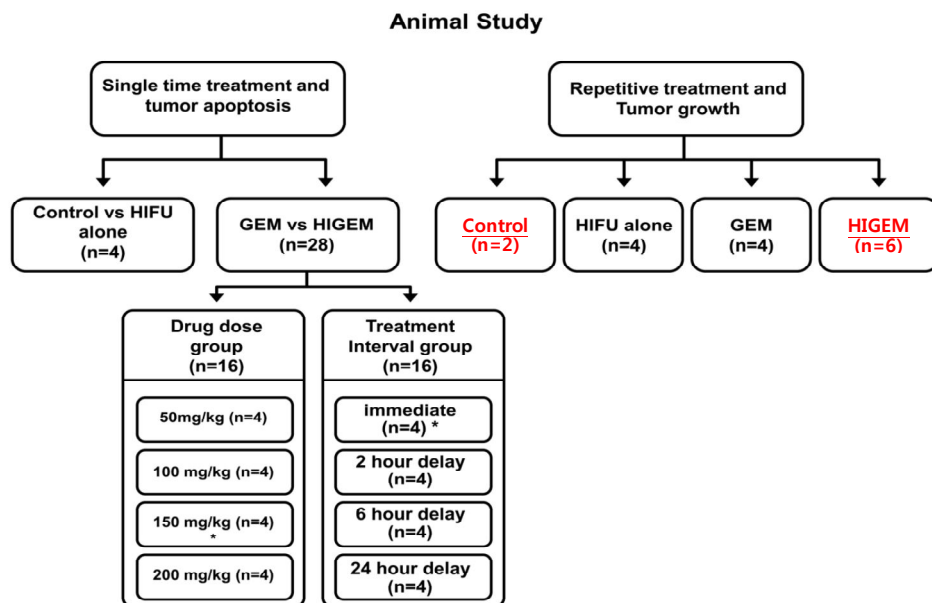
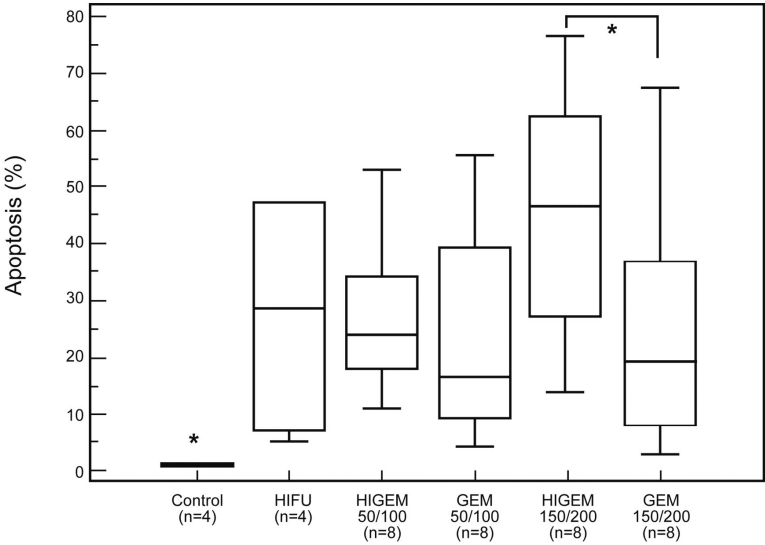


Fig. 4. Box plots of the apoptotic ratio (%) according to treatment. The line in each box represents the median, and the horizontal boundaries of the boxes represent the first and third quartiles. The vertical error bars show the minimum and maximum values (range).

A. The Kruskal-Wallis test shows that concurrent HIFU and gemcitabine treatment is significantly superior to gemcitabine treatment in generating apoptosis when high doses (150 & 200 mg/kg) of gemcitabine were used ($p = 0.01$). All treatment groups are significantly different in terms of apoptotic ratio compared with the control.

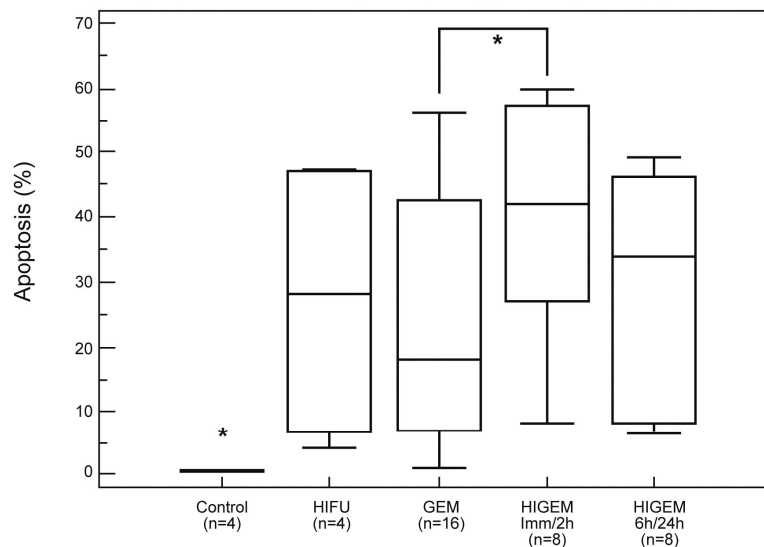


HIFU: high-intensity focused ultrasound, GEM: gemcitabine, HIGEM:

concurrent treatment with HIFU and gemcitabine, numbers in the second line:

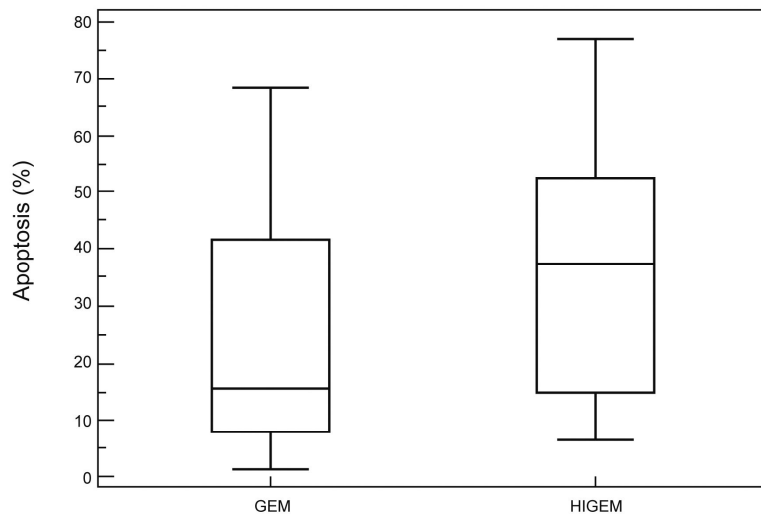
dosage of gemcitabine (mg/kg)

B. The Kruskal-Wallis test shows that concurrent HIFU and gemcitabine treatment is significantly superior to gemcitabine treatment in generating apoptosis when a short-term delay (immediate and 2-hour delay) was used ($p = 0.008$). All treatment groups are significantly different in terms of the apoptotic ratio compared with the control. The dose of gemcitabine was 150 mg/kg in all subgroups.



*HIFU: high-intensity focused ultrasound, GEM: gemcitabine, HIGEM:
concurrent treatment with HIFU and gemcitabine, Imm: immediately, H:
delayed hours after gemcitabine injection to HIFU treatment*

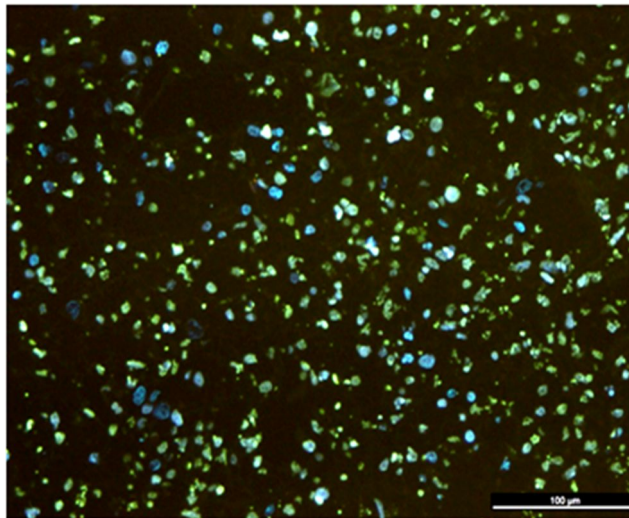
Fig. 5. A paired t-test shows that concurrent HIFU and gemcitabine treatment is significantly superior to gemcitabine treatment in generating apoptosis in 28 mice ($p = 0.02$).



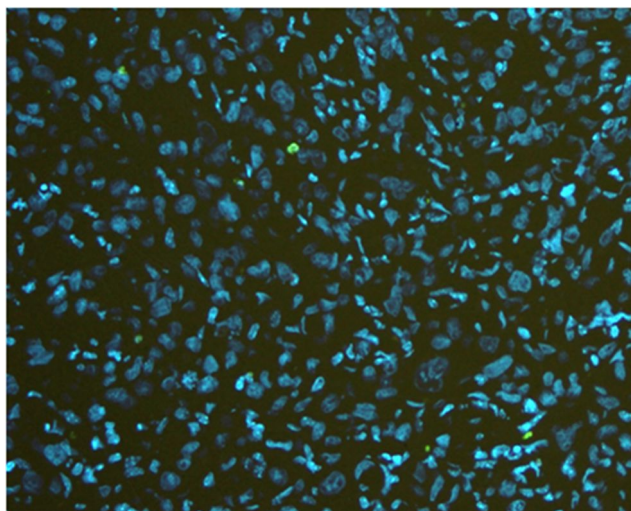
GEM: gemcitabine, HIGEM: concurrent treatment with HIFU and gemcitabine

Fig. 6. Fluorescent TUNEL assay with DAPI staining in single time treatment group, single individual, which was treated with 200 mg/kg of gemcitabine. (Blue: DAPI staining for dead cells, Green: TUNEL staining for apoptotic cells only)

A. Concurrent treatment with HIFU and gemcitabine 200 mg/kg

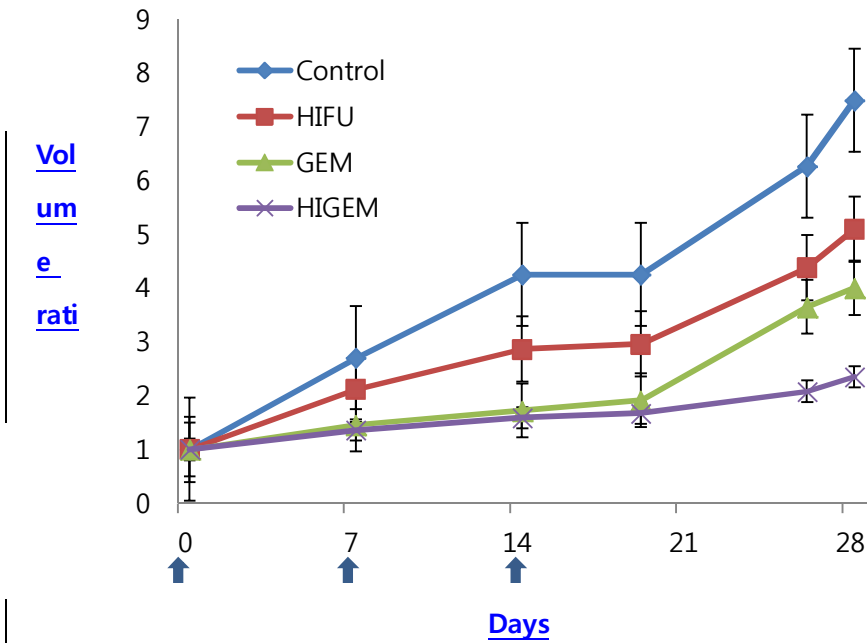


B. Treatment with gemcitabine 200 mg/kg only



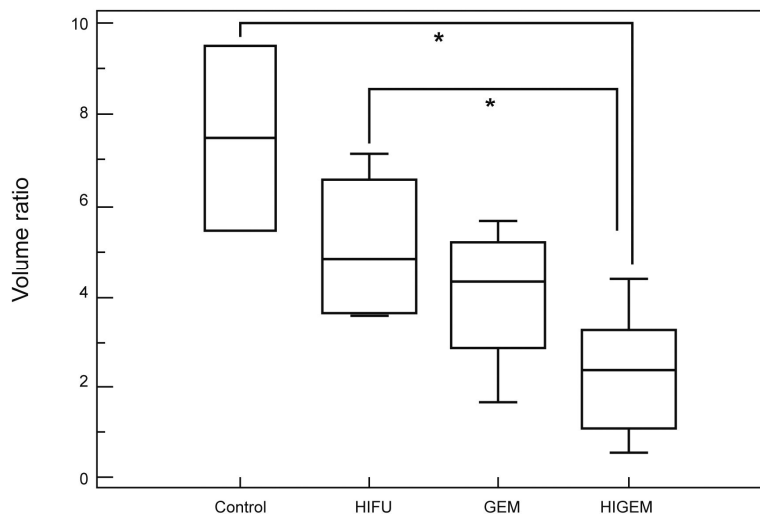
HIFU: high-intensity focused ultrasound. TUNEL: terminal deoxynucleotidyl transferase-mediated dUTP nick end labeling, DAPI: 4', 6-diamidino-2-phenylindole

Fig. 7. Line graph shows serial changes in volume ratio (tumor volume at day 28/ tumor volume at day 0) with weekly treatment for 3 consecutive weeks with HIFU and/or gemcitabine on PANC-1 xenografts in BALB/c nude mice. Data are mean values and error bars indicate standard error of mean. Blue arrows denote treatment days. The concurrent HIFU and gemcitabine group shows the slowest tumor growth among the 4 groups.



HIFU: high-intensity focused ultrasound, GEM: gemcitabine, HIGEM: concurrent treatment with HIFU and gemcitabine.

Fig. 8. Box plots of volume ratio (tumor volume at day 28/ tumor volume at day 0) according to treatment after weekly treatment for 3 consecutive weeks with HIFU and/or gemcitabine on PANC-1 xenografts in BALB/c nude mice. The line in each box represents the median, and the horizontal boundaries of the boxes represent the first and third quartiles. The vertical error bars show the minimum and maximum values (range). The Kruskal-Wallis test shows that the concurrent HIFU and gemcitabine treatment group is significantly superior to the control and HIFU groups in suppressing tumor growth ($p = 0.05$). However, no significant difference exists between the concurrent group and the gemcitabine alone group despite a visible difference.



*HIFU: high-intensity focused ultrasound, GEM: gemcitabine, HIGEM:
concurrent treatment with HIFU and gemcitabine*

References

1. Hariharan D, Saied A, Kocher HM. Analysis of mortality rates for pancreatic cancer across the world. *HPB (Oxford)*. 2008;**10**(1):58-62.
2. Cardenes HR, Chiorean EG, Dewitt J, Schmidt M, Loehrer P. Locally advanced pancreatic cancer: current therapeutic approach. *Oncologist*. 2006;**11**(6):612-23.
3. Burris HA, 3rd, Moore MJ, Andersen J, et al. Improvements in survival and clinical benefit with gemcitabine as first-line therapy for patients with advanced pancreas cancer: a randomized trial. *J Clin Oncol*. 1997;**15**(6):2403-13.
4. Merl MY, Li J, Saif MW. The first-line treatment for advanced pancreatic cancer. Highlights from the "2010 ASCO Gastrointestinal Cancers Symposium". Orlando, FL, USA. January 22-24, 2010. *JOP*. 2010;**11**(2):148-50.
5. Gianfelice D, Khiat A, Amara M, Belblidia A, Boulanger Y. MR imaging-guided focused US ablation of breast cancer: histopathologic assessment of effectiveness-- initial experience. *Radiology*. 2003;**227**(3):849-

55.

6. Thuroff S, Chaussy C, Vallancien G, et al. High-intensity focused ultrasound and localized prostate cancer: efficacy results from the European multicentric study. *J Endourol*. 2003;**17**(8):673-7.

7. Wu F, Wang ZB, Chen WZ, Bai J, Zhu H, Qiao TY. Preliminary experience using high intensity focused ultrasound for the treatment of patients with advanced stage renal malignancy. *J Urol*. 2003;**170**(6 Pt 1):2237-40.

8. Kennedy JE, Wu F, ter Haar GR, et al. High-intensity focused ultrasound for the treatment of liver tumours. *Ultrasonics*. 2004;**42**(1-9):931-5.

9. Wu F, Wang ZB, Chen WZ, et al. Extracorporeal focused ultrasound surgery for treatment of human solid carcinomas: early Chinese clinical experience. *Ultrasound Med Biol*. 2004;**30**(2):245-60.

10. Kennedy JE. High-intensity focused ultrasound in the treatment of solid tumours. *Nat Rev Cancer*. 2005;**5**(4):321-7.

11. Wu F, Wang ZB, Zhu H, et al. Feasibility of US-guided high-intensity focused ultrasound treatment in patients with advanced pancreatic cancer: initial experience. *Radiology*. 2005;**236**(3):1034-40.

12. Xiong LL, Hwang JH, Huang XB, et al. Early clinical experience using high intensity focused ultrasound for palliation of inoperable pancreatic cancer. JOP. 2009;**10**(2):123-9.
13. Chen W, Zhu H, Zhang L, et al. Primary bone malignancy: effective treatment with high-intensity focused ultrasound ablation. Radiology. 2010;**255**(3):967-78.
14. Yuh EL, Shulman SG, Mehta SA, et al. Delivery of systemic chemotherapeutic agent to tumors by using focused ultrasound: study in a murine model. Radiology. 2005;**234**(2):431-7.
15. Frenkel V, Etherington A, Greene M, et al. Delivery of liposomal doxorubicin (Doxil) in a breast cancer tumor model: investigation of potential enhancement by pulsed-high intensity focused ultrasound exposure. Acad Radiol. 2006;**13**(4):469-79.
16. Dromi S, Frenkel V, Luk A, et al. Pulsed-high intensity focused ultrasound and low temperature-sensitive liposomes for enhanced targeted drug delivery and antitumor effect. Clin Cancer Res. 2007;**13**(9):2722-7.
17. Kim YS, Rhim H, Choi MJ, Lim HK, Choi D. High-intensity focused ultrasound therapy: an overview for radiologists. Korean J Radiol.

2008;**9**(4):291-302.

18. Poff JA, Allen CT, Traugher B, et al. Pulsed high-intensity focused ultrasound enhances apoptosis and growth inhibition of squamous cell carcinoma xenografts with proteasome inhibitor bortezomib. *Radiology*. 2008;**248**(2):485-91.

19. Zhao H, Yang G, Wang D, et al. Concurrent gemcitabine and high-intensity focused ultrasound therapy in patients with locally advanced pancreatic cancer. *Anticancer Drugs*. 2010;**21**(4):447-52.

20. Cao H, Xu Z, Long H, et al. Transcatheter arterial chemoembolization in combination with high-intensity focused ultrasound for unresectable hepatocellular carcinoma: a systematic review and meta-analysis of the chinese literature. *Ultrasound Med Biol*. 2011;**37**(7):1009-16.

21. Jin C, Zhu H, Wang Z, et al. High-intensity focused ultrasound combined with transarterial chemoembolization for unresectable hepatocellular carcinoma: long-term follow-up and clinical analysis. *Eur J Radiol*. 2011;**80**(3):662-9.

22. Lee JY, Choi BI, Ryu JK, et al. Concurrent chemotherapy and pulsed high-intensity focused ultrasound therapy for the treatment of unresectable

- pancreatic cancer: initial experiences. Korean J Radiol. 2011;**12**(2):176-86.
23. Mu Z, Ma CM, Chen X, Cvetkovic D, Pollack A, Chen L. MR-guided pulsed high intensity focused ultrasound enhancement of docetaxel combined with radiotherapy for prostate cancer treatment. Phys Med Biol. 2012;**57**(2):535-45.
24. Yang FY, Teng MC, Lu M, et al. Treating glioblastoma multiforme with selective high-dose liposomal doxorubicin chemotherapy induced by repeated focused ultrasound. Int J Nanomedicine. 2012;**7**:965-74.
25. Wang RS, Liu LX, Gu YH, Lin QF, Guo RH, Shu YQ. The effect of endostatin and gemcitabine combined with HIFU on the animal xenograft model of human pancreatic cancer. Biomed Pharmacother. 2010;**64**(5):309-12.
26. Coussios CC, Farny CH, Haar GT, Roy RA. Role of acoustic cavitation in the delivery and monitoring of cancer treatment by high-intensity focused ultrasound (HIFU). Int J Hyperthermia. 2007;**23**(2):105-20.
27. Datta S, Coussios CC, Ammi AY, Mast TD, de Courten-Myers GM, Holland CK. Ultrasound-enhanced thrombolysis using Definity as a cavitation nucleation agent. Ultrasound Med Biol. 2008;**34**(9):1421-33.
28. Hancock HA, Smith LH, Cuesta J, et al. Investigations into pulsed

high-intensity focused ultrasound-enhanced delivery: preliminary evidence for a novel mechanism. *Ultrasound Med Biol.* 2009;**35**(10):1722-36.

29. Hynynen K, Clement G. Clinical applications of focused ultrasound-the brain. *Int J Hyperthermia.* 2007;**23**(2):193-202.

30. Bazan-Peregrino M, Arvanitis CD, Rifai B, Seymour LW, Coussios CC. Ultrasound-induced cavitation enhances the delivery and therapeutic efficacy of an oncolytic virus in an in vitro model. *J Control Release.* 2012;**157**(2):235-42.

31. Rifai B, Arvanitis CD, Bazan-Peregrino M, Coussios CC. Cavitation-enhanced delivery of macromolecules into an obstructed vessel. *J Acoust Soc Am.* 2010;**128**(5):EL310-15.

32. Pan H, Zhou Y, Sieling F, Shi J, Cui J, Deng C. Sonoporation of cells for drug and gene delivery. *Conf Proc IEEE Eng Med Biol Soc.* 2004;**5**:3531-4.

33. Wu J, Pepe J, Rincon M. Sonoporation, anti-cancer drug and antibody delivery using ultrasound. *Ultrasonics.* 2006;**44 Suppl 1**:e21-5.

34. Iwanaga K, Tominaga K, Yamamoto K, et al. Local delivery system of cytotoxic agents to tumors by focused sonoporation. *Cancer Gene Ther.*

2007;**14**(4):354-63.

35. Maeda H, Tominaga K, Iwanaga K, et al. Targeted drug delivery system for oral cancer therapy using sonoporation. *J Oral Pathol Med.* 2009;**38**(7):572-9.

36. Miller DL, Dou C. Induction of apoptosis in sonoporation and ultrasonic gene transfer. *Ultrasound Med Biol.* 2009;**35**(1):144-54.

37. O'Neill BE, Vo H, Angstadt M, Li KP, Quinn T, Frenkel V. Pulsed high intensity focused ultrasound mediated nanoparticle delivery: mechanisms and efficacy in murine muscle. *Ultrasound Med Biol.* 2009;**35**(3):416-24.

38. Liang HD, Tang J, Halliwell M. Sonoporation, drug delivery, and gene therapy. *Proc Inst Mech Eng H.* 2010;**224**(2):343-61.

39. Lee NG, Berry JL, Lee TC, et al. Sonoporation enhances chemotherapeutic efficacy in retinoblastoma cells in vitro. *Invest Ophthalmol Vis Sci.* 2011;**52**(6):3868-73.

40. Yang F, Gu N, Chen D, et al. Experimental study on cell self-sealing during sonoporation. *J Control Release.* 2008;**131**(3):205-10.

41. Jung SE, Cho SH, Jang JH, Han JY. High-intensity focused ultrasound ablation in hepatic and pancreatic cancer: complications. *Abdom*

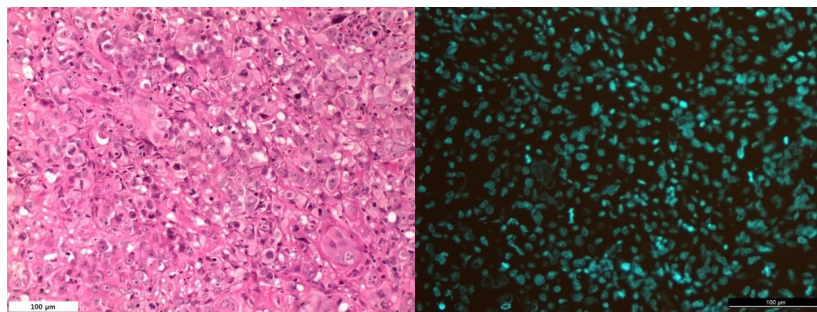
Imaging. 2011;**36**(2):185-95.

42. Chen ZY, Liang K, Qiu RX, Luo LP. Enhancing microRNA transfection to inhibit survivin gene expression and induce apoptosis: could it be mediated by a novel combination of sonoporation and polyethylenimine? Chin Med J (Engl). 2011;**124**(21):3592-4.

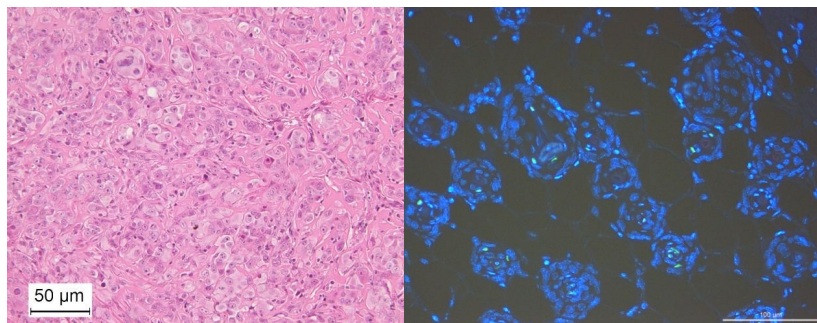
Appendix

1. Representative figures of H & E staining (left) and fluorescent TUNEL assay (right, apoptotic cells were stained in green) in each subgroup after single time treatment.

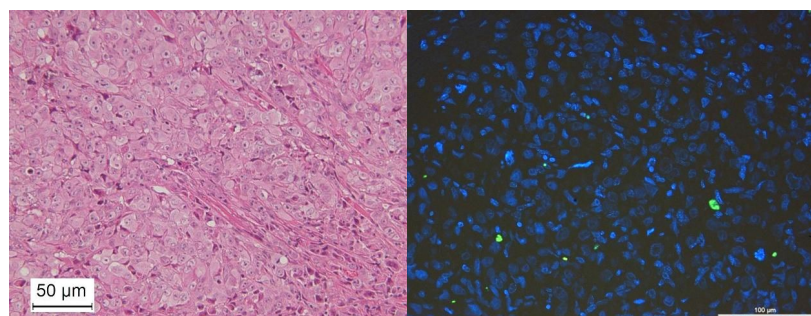
A. Control



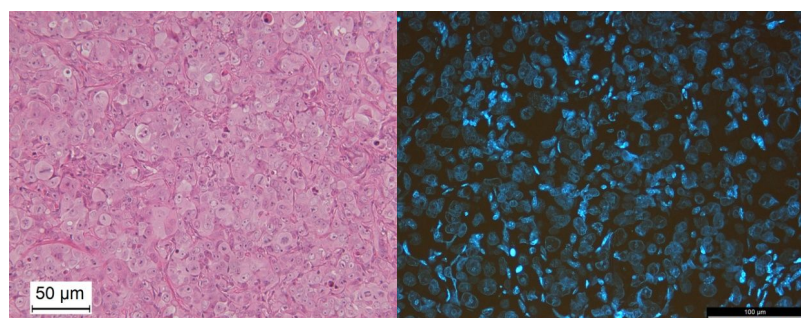
B. HIFU only



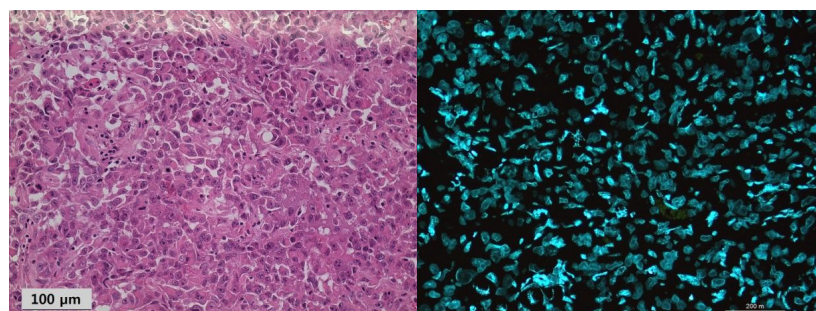
C. HIGEM 50 mg/Kg



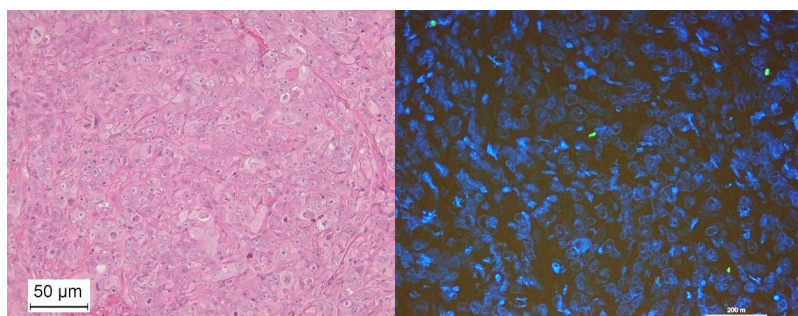
D. GEM 50 mg/Kg



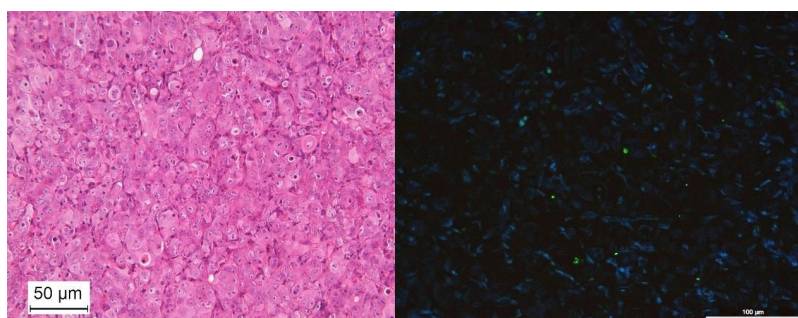
E. HIGEM 100 mg/Kg



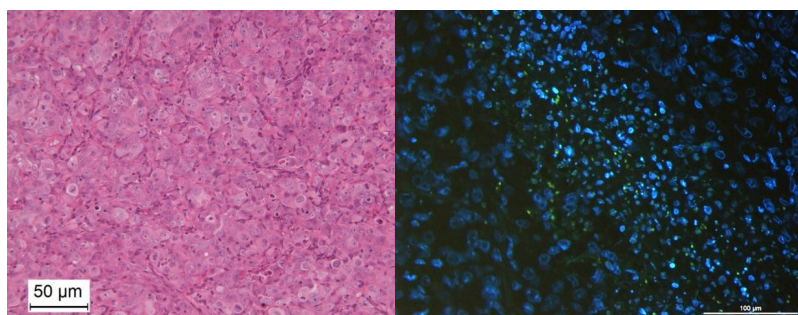
F. GEM 100 mg/Kg



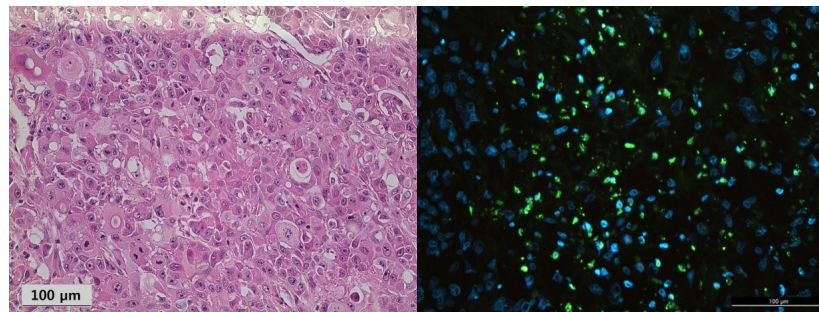
G. HIGEM 150 mg/Kg



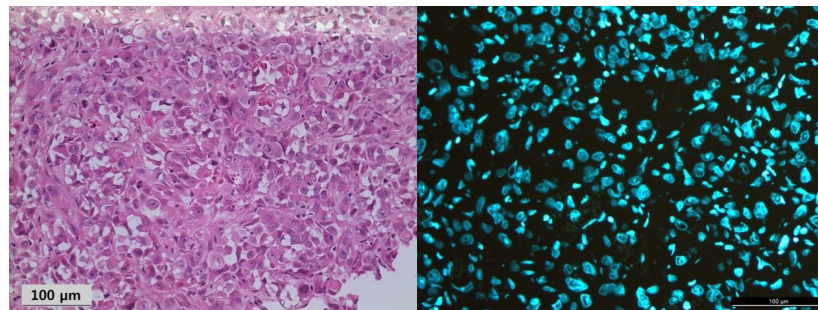
H. GEM 150 mg/Kg



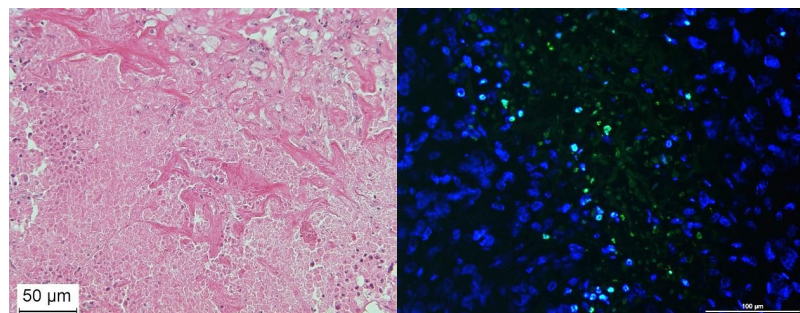
I. HIGEM 200 mg/Kg



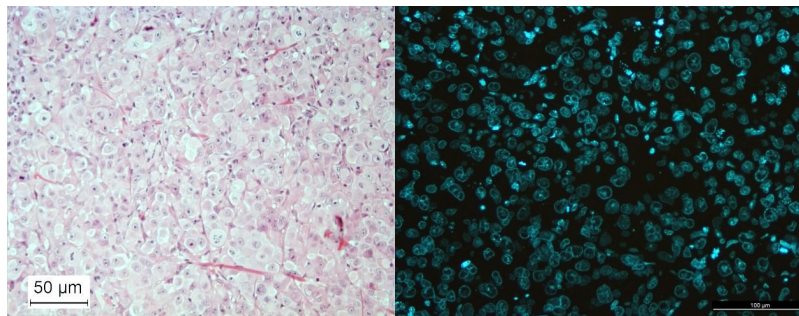
J. GEM 200 mg/Kg



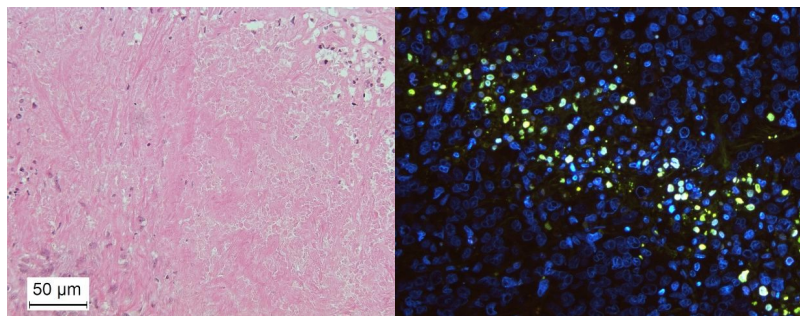
K. HIGEM 2-hour delay



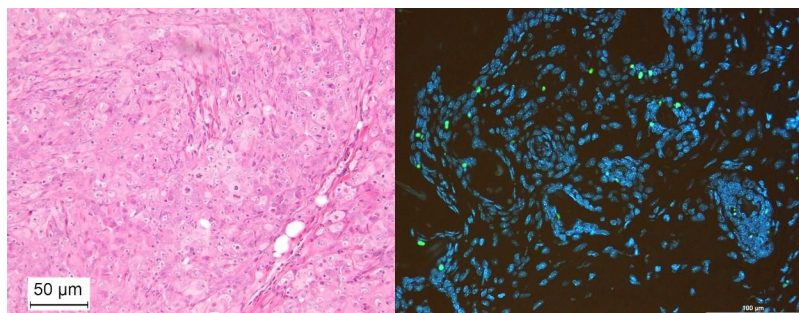
L. GEM 2-hour delay



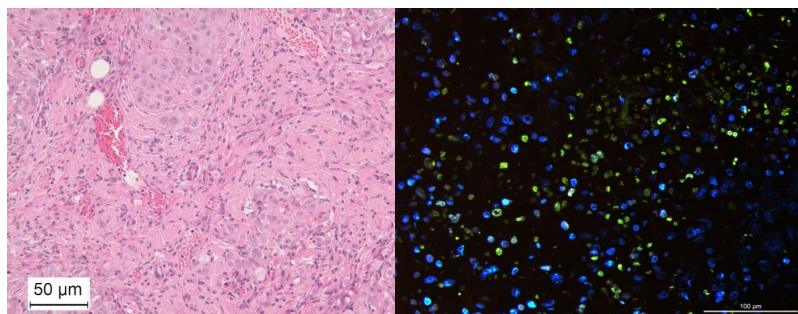
M. HIGEM 6-hour delay



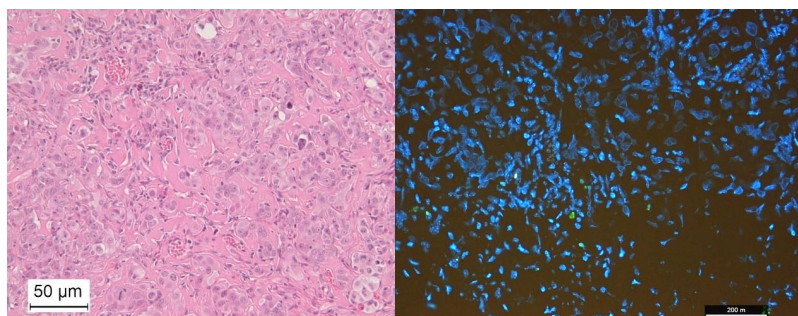
N. GEM 6-hour delay



O. HIGEM 24-hour delay



P. GEM 24-hour delay

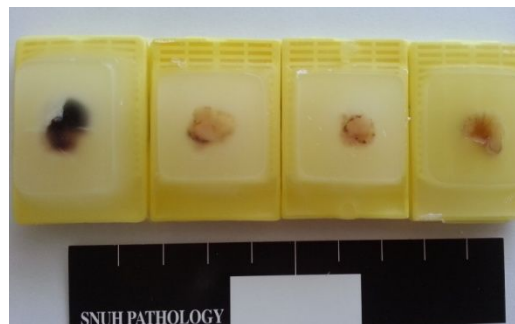


2. Obtained specimen with representative figures of H & E staining after 3-time repetitive treatment in each subgroup.

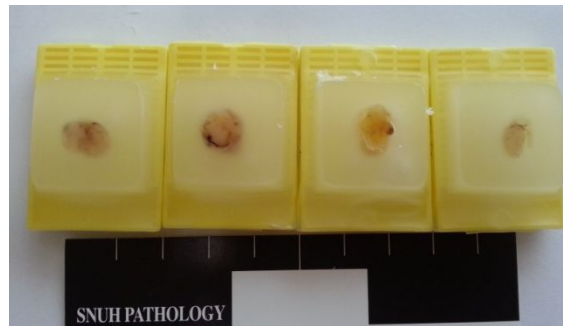
A. Control



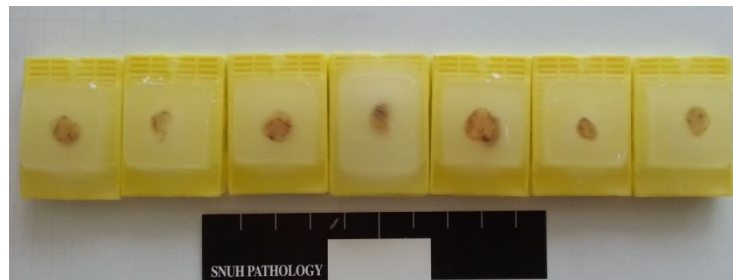
B. HIFU only



C. GEM



D. HIGEM



HIFU: high-intensity focused ultrasound, GEM: gemcitabine, HIGEM: concurrent treatment with HIFU and gemcitabine

초 록

서론: 췌장암에서 고강도 집속 초음파 (high-intensity focused ultrasound, HIFU)와 항암제 gemcitabine의 병용 요법이 세포자멸사를 촉진시킬 수 있는지에 대해 알아보기로 하였다.

방법: BALB/c 누드마우스의 피하 조직에 인간 췌장암 세포 (PANC-1)를 이식하여 췌장암 동물 모델을 만들었다. 첫 실험에서 누드마우스들은 다음의 네 군으로 무작위로 나뉘었다; 대조군 (n=4), HIFU 치료만 받은 군 (n=4), gemcitabine 치료만 받은 군 (GEM) (n=28), HIFU와 gemcitabine의 병용 치료를 받은 군 (HIGEM) (n=28). GEM과 HIGEM군은 약물 용량 (50 - 200 mg/kg) 및 HIFU 치료와 gemcitabine 주사 시간 간격 (즉시 - 24시간 후)에 따라 각각 4개의 아군으로 나뉘었다. 세포자멸사 비율은 terminal deoxynucleotidyl transferase-mediated dUTP nick end-labeling (TUNEL)기법을 이용하여, 조직 괴사율은 Harris hematoxylin solution and eosin Y (H & E)염색을 통해 실험 3일 후 측정하였다. 두 번째 실험에서는 각 치료군에서 종양의 성장 속도를 알아보았다. 각 실험군은 3주 동안 1주 간격으로 치료를 받은 후 한달 동안 정기적으로 종양의 크기를 측정하였다.

결과: 첫 실험에서 종합적인 세포자멸사 비율은 HIGEM군이 GEM군보다 통계적으로 유의하게 높았다 ($p=0.02$). 각 아군들을 분석했을 때 고용량(150–200 mg/kg)의 gemcitabine을 사용한 HIGEM 아군이, 또한 HIFU와 gemcitabine의 주입 간격이 짧은 HIGEM 아군(2시간 이내)이 통계적으로 유의하게 GEM군에 비해 우월한 치료 효과를 보였다 ($p=0.01$). 두 번째 실험에서는 HIGEM군이 가장 느린 종양 성장 속도를 보였다. 그러나 HIGEM군과 GEM군 사이의 통계적 유의성은 없었다 ($p>0.05$).

결론: HIFU와 gemcitabine의 병용 요법은 췌장암의 세포자멸사를 촉진하고, 종양 성장을 억제하는데 효과가 있었다. 이러한 병용 요법을 위해서는 고용량 gemcitabine과 짧은 간격의 HIFU와 항암 치료가 추천된다.

주요 단어

고강도 집속 초음파

췌장암

Gemcitabine

동물 연구

학번: 2011-30570